Supplementary Material for

Nutrient co-limitation in the subtropical western North Pacific

Thomas J. Browning*, Xin Liu, Ruifeng Zhang, Zuozhu Wen, Jing Liu, Yaqian Zhou, Feipeng Xu, Yihua Cai, Kuanbo Zhou, Zhimian Cao, Yuanli Zhu, Dalin Shi, Eric P. Achterberg, Minhan Dai

*Corresponding author. Email: tbrowning@geomar.de

This file includes:

Supplementary Text 1 and 2
Figs. S1 to S7
Tables S1
Supplementary References

Supplementary Text

Supplementary Text 1: Form of N supply

As indicated in Figure 1c, at eight of the experimental sites, the N and N + Fe treatments were supplied with the N addition in the form of nitrate alone (2 μM) or nitrate plus ammonium (1 μM + 1 μM). Some strains of *Prochlorococcus* cannot utilize nitrate as an N source and therefore reduced *Prochlorococcus* growth following supply of nitrate alone was hypothesized (Moore et al., 2002; Martiny et al., 2009; Berube et al., 2015; Berthelot et al., 2019). Furthermore, nitrate uptake by all phytoplankton is mediated by the Fe-requiring enzyme nitrate reductase; therefore, at N limited sites, supply of Fe alongside the nitrate was hypothesized to enhance growth (Raven et al., 1990). No significant differences in cell concentrations of *Prochlorococcus*, *Synechococcus*, or picophytoplankton were observed between N supplied as nitrate or nitrate plus ammonium (or the corresponding N+Fe treatments; Fig. 2a). *Prochlorococcus* fluorescence per cell, a proxy for chlorophyll-a per cell, was however higher following supply of N added as nitrate plus ammonia over nitrate alone, suggesting that N limitation of pigment synthesis for this species was relieved to a greater extent when N was supplied as ammonia (Fig. 2a). Overall, these results suggested that the form of N supply was not a key determinant of phytoplankton responses, but appeared to have a physiological impact on *Prochlorococcus* in terms of pigment synthesis and potentially associated growth rates (Cavender-Bares et al., 1999; Mann et al., 2000).

Supplementary Text 2: Resource competition model response to varying Fe:N supply ratio

The resource competition model of Ward et al. (2013) was used to evaluate the impact of varying Fe:N supply ratios on competition between diazotrophic and non-diazotrophic phytoplankton and the emergent (co-)limiting nutrients for the system (Fig. S7). In the model, diazotrophic phytoplankton compete with non-diazotroph phytoplankton for nutrients (N, P, and Fe) under grazing pressure. Mixing with deep waters entrains nutrients and dilutes phytoplankton. Aerosol deposition supplies additional Fe to surface waters. The supply ratio of Fe:N was modified by varying the N concentration of the deep water entrained into the surface layer and the Fe aerosol flux. As in Ward et al. (2013), the Fe:N supply ratio was calculated and displayed in Figure S7 normalized to phytoplankton Fe:N requirements ($\phi_{Fe:N}$):

$$\phi_{\mathrm{Fe:N}} = \frac{\kappa Fe_0 + f_{atm}}{\kappa N_0} r_{pFe}^{-1},$$

where κ is the mixing coefficient (d^{-1}), N_0 and Fe_0 are deep water N and Fe concentrations respectively, f_{atm} is the atmospheric Fe aerosol flux, and r_{pFe} is the non-diazotrophic phytoplankton Fe:N ratio. Model variables and parameters are shown in Table S1; for the model equations see Ward et al. (2013). Diazotroph and non-diazotroph growth rates, half saturation constants for nitrate, phosphate, and Fe, P:N ratios, and Fe:N ratios were identical to those used in Ward et al. (2013). Deep water (i.e., below mixed layer) nitrate concentrations encompassed a range reflecting our observations (Table S1; Fig. S6) but also including the values used by Ward et al. (2013). Deep water P concentrations were simply set to deep-water nitrate/10, broadly reflecting observations at ~100–200 m. Deep water dissolved Fe concentrations were fixed to those similar to observations (0.2 nM; Fig. S6). Aerosol Fe deposition encompassed a range within that used by Schlosser et al. (2014) (although to a lower maximum value reflecting the lower level of aerosol deposition in the Western North Pacific system).

At each Fe:N supply ratio, the model was run to steady state (that is, non-varying phytoplankton and nutrient concentrations). Steady state values of biomass and nutrients were plotted (Fig. S7) and used to initiate 48 h simulations following nutrient enrichment. In the latter simulations, nutrients were simply added in the various combinations used in the bioassay experiments and the phytoplankton growth simulations proceeded with exactly the same equations and parameterization (except no dilution/mixing term) for the previously described model (Fig. S7). The fractional change in biomass for +P+N and +Fe+N treatments relative to +N were then calculated (Fig. S7e and j).

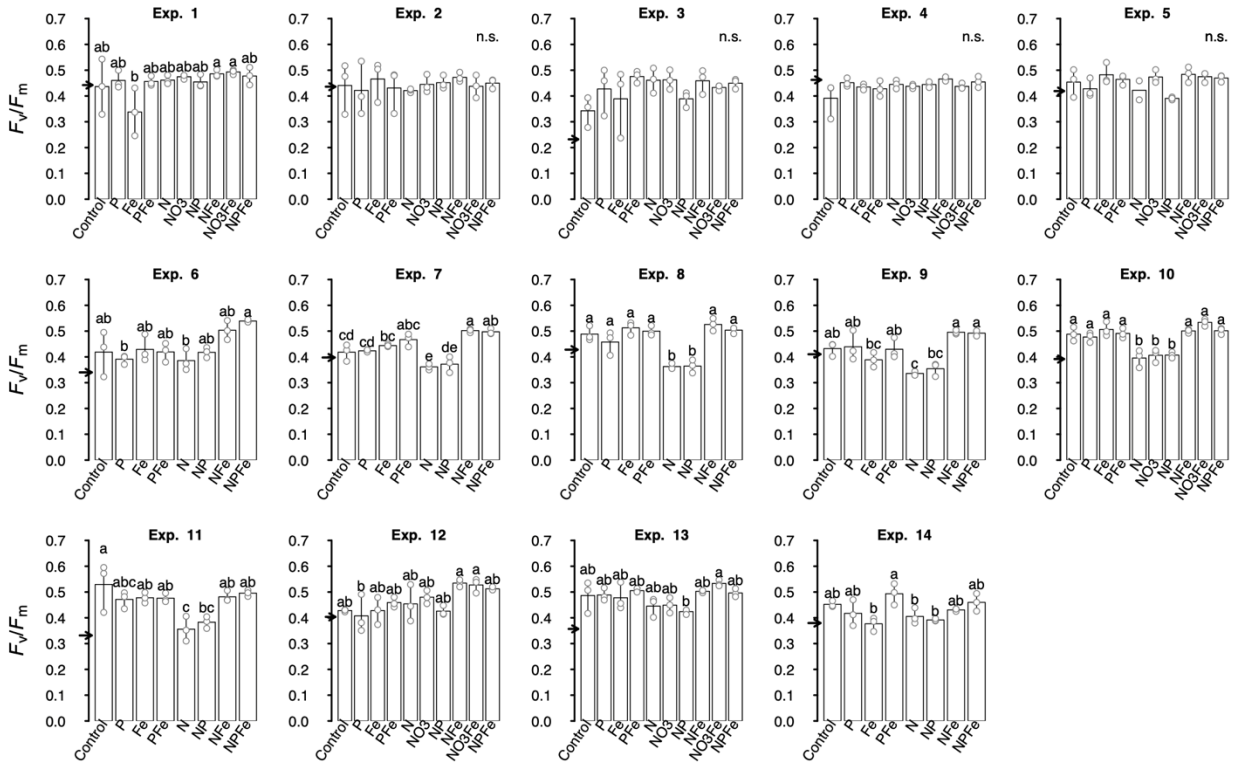

Fig. S1. F_v/F_m changes in the experiments. Bars are mean of triplicate biological replicates, with individual values indicated as points. Arrows point to mean initial values. Bars labelled with the same letter have statistically indistinguishable means between treatments (one-way ANOVA, α=0.05, followed by Tukey posthoc test; n.s.=not significant).

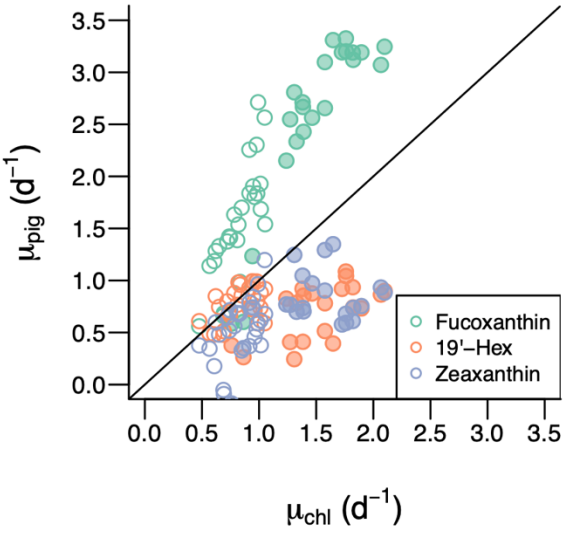

Fig. S2. Net growth rates of three diagnostic pigments in experiments relative to chlorophyll-a (1:1 line shown). 19'–Hex is 19'–Hexanoyloxyfucoxanthin. Filled circles are for 'N+Fe' or 'N+P+Fe' treatments.

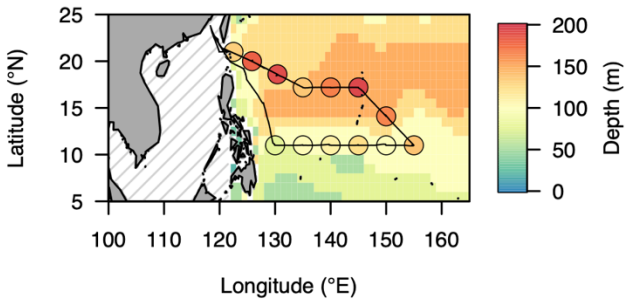

Fig. S3. Spatial gradients in nitracline depths as derived from the world ocean atlas climatology (background) and cruise observations (points).

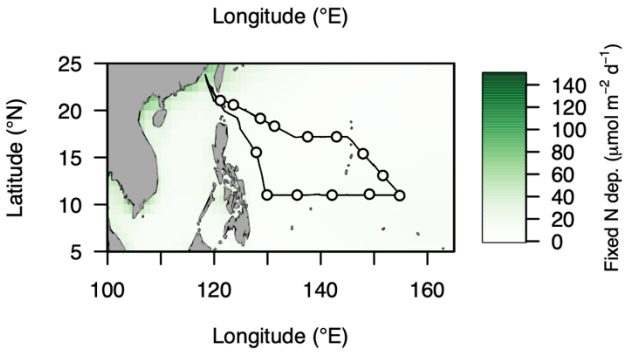

Fig. S4. Modelled climatological aerosol deposition of fixed nitrogen for May–June from Chien et al. (2016).

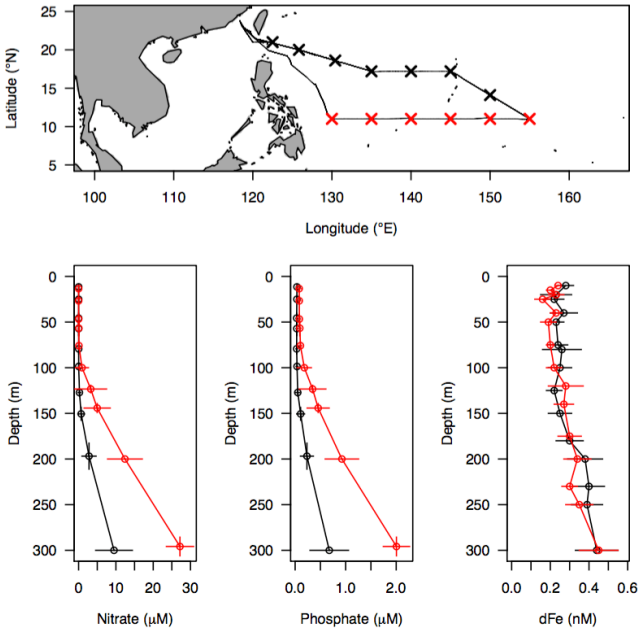

Fig. S5. Vertical nutrient distributions. Average vertical distributions of nitrate (here representing nitrate+nitrite), phosphate, and dissolved Fe (dFe) measured at northern and southern stations on the KK1903 cruise (identified as cross symbols in map). Error bars show the standard deviation of measurements across stations.

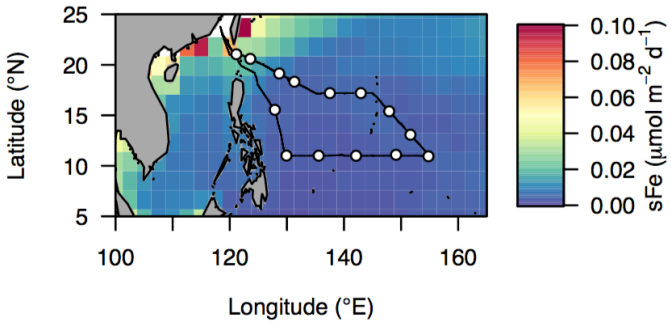

Fig. S6. Modelled climatological soluble Fe (sFe) deposition rate for May–June from Chien et al. (2016).

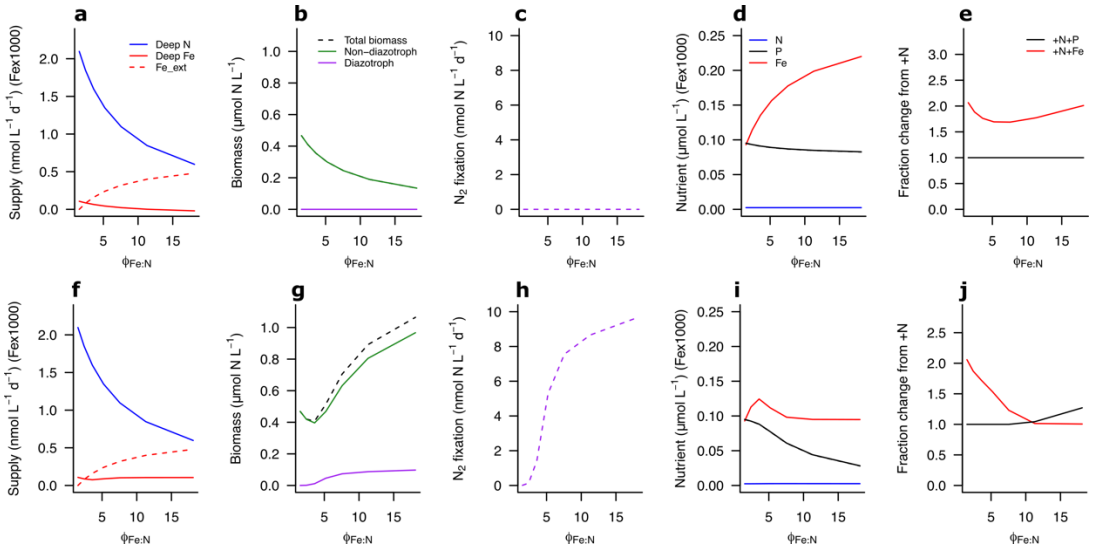

Fig. S7. Development of serial limitation categories in a resource competition model (Ward et al., 2013). The model contains diazotrophic and non-diazotrophic phytoplankton competing for nutrients under varying, normalized N:Fe supply, $\phi_{Fe:N}$ (See Supplementary Text 2 for further details and Table S1 for model variables and parameters). $\phi_{Fe:N}$ was varied by altering the deep N concentration and external Fe supply (Fe_ext; representing input from aerosols for example) as shown in panels '**a**' and '**f**'. Deep water P varied with deep water N at a constant ratio, whilst deep-water Fe was kept constant. Upper panels **a**–**e** are for a 'no diazotroph' case, lower panels are for a 'with diazotrophs' case. Plots show steady state model solutions for each value of $\phi_{Fe:N}$: biomass concentrations (**b**, **g**); N_2 fixation rates (**c**, **h**); nutrient concentrations (**d**, **i**). Panels '**e**' and '**j**' indicate the fractional change in steady state biomass after 48 h when amended in the model with either N + P or N + Fe, relative to amendment with N alone (i.e., as in the experiments conducted on the cruise). In the case with no diazotrophs (upper panels) phytoplankton are singly limited by N and serially limited by Fe across all values of $\phi_{Fe:N}$. In the case with diazotrophs (lower panels) phytoplankton are also always singly limited by N, but there is a switch from serial limitation by Fe at low $\phi_{Fe:N}$ to serial limitation by P at higher $\phi_{Fe:N}$, as the supply ratio of Fe:N increasingly favors diazotrophs, enhancing N_2 fixation, and drawing down the available P to serially limiting levels.

Table S1. Variables/parameters for the resource competition model.

Variable/Parameter	Value(s)
Deep water nitrate (μM)	0.6–2.1
Deep water phosphate (μM)	0.06–0.21
Deep water Fe (nM)	0.2
Atmospheric Fe supply (pM d^{-1})	0–0.48
Mixing coefficient (d^{-1})	0.001
Non-diazotroph maximum growth rate (d^{-1})	2.5
Non-diazotroph half-saturation constant for nitrate (μM)	0.056
Non-diazotroph half-saturation constant for phosphate (μM)	0.035
Non-diazotroph half-saturation constant for Fe (nM)	0.35
Non-diazotroph P:N ratio	0.0625
Non-diazotroph Fe:N ratio	6.25×10^{-5}
Diazotroph maximum growth rate (d^{-1})	1.25
Diazotroph half-saturation constant for phosphate (μM)	0.035
Diazotroph half-saturation constant for Fe (nM)	1.1
Diazotroph P:N ratio	0.025
Diazotroph Fe:N ratio	7.5×10^{-4}
Mortality rate (d^{-1})	0.1

References

Berthelot, H., Duhamel, S., L'Helguen, S., Maguer, J.F., Wang, S., Cetinić, I. and Cassar, N., 2019. NanoSIMS single cell analyses reveal the contrasting nitrogen sources for small phytoplankton. *ISME* **13**, 651-662.

Berube, P.M., Biller, S.J., Kent, A.G., Berta-Thompson, J.W., Roggensack, S.E., Roache-Johnson, K.H., Ackerman, M., Moore, L.R., Meisel, J.D., Sher, D. and Thompson, L.R., 2015. Physiology and evolution of nitrate acquisition in Prochlorococcus. *ISME* **9**, 1195-1207.

Cavender-Bares, K.K., Mann, E.L., Chisholm, S.W., Ondrusek, M.E. and Bidigare, R.R., 1999. Differential response of equatorial Pacific phytoplankton to iron fertilization. *Limnol. Oceanogr.* **44**, 237-246.

Chien, C.T., Mackey, K.R., Dutkiewicz, S., Mahowald, N.M., Prospero, J.M. and Paytan, A., 2016. Effects of African dust deposition on phytoplankton in the western tropical Atlantic Ocean off Barbados. *Global Biogeochem. Cy.* **30**, 716-734.

Mann, E.L. and Chisholm, S.W., 2000. Iron limits the cell division rate of Prochlorococcus in the eastern equatorial Pacific. *Limnol. Oceanogr.* **45**, 1067-1076.

Martiny, A.C., Kathuria, S. and Berube, P.M., 2009. Widespread metabolic potential for nitrite and nitrate assimilation among Prochlorococcus ecotypes. *Proc. Nat. Acad. Sci. USA*, **106**, 10787-10792.

Moore, L.R., Post, A.F., Rocap, G. and Chisholm, S.W., 2002. Utilization of different nitrogen sources by the marine cyanobacteria Prochlorococcus and Synechococcus. *Limnol. Oceanogr.* **47**, 989-996.

Raven, J.A., 1990. Predictions of Mn and Fe use efficiencies of phototrophic growth as a function of light availability for growth and of C assimilation pathway. *New Phytologist* **116**, 1-18.

Schlosser, C., Klar, J.K., Wake, B.D., Snow, J.T., Honey, D.J., Woodward, E.M.S., Lohan, M.C., Achterberg, E.P. and Moore, C.M., 2014. Seasonal ITCZ migration dynamically controls the location of the (sub) tropical Atlantic biogeochemical divide. *Proc. Nat. Acad. Sci.* **111**, 1438-1442.

Ward, B.A., Dutkiewicz, S., Moore, C.M. and Follows, M.J., 2013. Iron, phosphorus, and nitrogen supply ratios define the biogeography of nitrogen fixation. *Limnol. Oceanogr.* **58**, 2059-2075.